



Journal of Geophysical Research: Earth Surface

RESEARCH ARTICLE

10.1002/2015JF003602

Key Points:

- Ground ice occupies a large volume of the top 3 m of Arctic permafrost
- Ice wedge thawing creates positive feedbacks that enhance degradation
- Ecological responses provide negative feedbacks that stabilize the surface

Supporting Information:

• Figures S1-S5

Correspondence to:

M. T. Jorgenson, ecoscience@alaska.net

Citation:

Jorgenson, M. T., M. Kanevskiy, Y. Shur, N. Moskalenko, D. R. N. Brown, K. Wickland, R. Striegl, and J. Koch (2015), Role of ground ice dynamics and ecological feedbacks in recent ice wedge degradation and stabilization, J. Geophys. Res. Earth Surf., 120, doi:10.1002/2015JF003602.

Received 1 MAY 2015 Accepted 11 OCT 2015 Accepted article online 15 OCT 2015

Role of ground ice dynamics and ecological feedbacks in recent ice wedge degradation and stabilization

M. T. Jorgenson¹, M. Kanevskiy², Y. Shur², N. Moskalenko³, D. R. N. Brown⁴, K. Wickland⁵, R. Striegl⁵, and J. Koch⁶

¹Alaska Ecoscience, Fairbanks, Alaska, USA, ²Institute of Northern Engineering, University of Alaska Fairbanks, Fairbanks, Alaska, USA, ³Institute of the Earth Cryosphere of SB RAS, Moscow State University, Moscow, Russia, ⁴Department of Biology and Wildlife, University of Alaska Fairbanks, Fairbanks, Alaska, USA, ⁵U.S. Geological Survey, Boulder, Colorado, USA, ⁶U.S. Geological Survey, Anchorage, Alaska, USA

Abstract Ground ice is abundant in the upper permafrost throughout the Arctic and fundamentally affects terrain responses to climate warming, Ice wedges, which form near the surface and are the dominant type of massive ice in the Arctic, are particularly vulnerable to warming. Yet processes controlling ice wedge degradation and stabilization are poorly understood. Here we quantified ice wedge volume and degradation rates, compared ground ice characteristics and thermal regimes across a sequence of five degradation and stabilization stages and evaluated biophysical feedbacks controlling permafrost stability near Prudhoe Bay, Alaska. Mean ice wedge volume in the top 3 m of permafrost was 21%. Imagery from 1949 to 2012 showed thermokarst extent (area of water-filled troughs) was relatively small from 1949 (0.9%) to 1988 (1.5%), abruptly increased by 2004 (6.3%) and increased slightly by 2012 (7.5%). Mean annual surface temperatures varied by 4.9°C among degradation and stabilization stages and by 9.9°C from polygon center to deep lake bottom. Mean thicknesses of the active layer, ice-poor transient layer, ice-rich intermediate layer, thermokarst cave ice, and wedge ice varied substantially among stages. In early stages, thaw settlement caused water to impound in thermokarst troughs, creating positive feedbacks that increased net radiation, soil heat flux, and soil temperatures. Plant growth and organic matter accumulation in the degraded troughs provided negative feedbacks that allowed ground ice to aggrade and heave the surface, thus reducing surface water depth and soil temperatures in later stages. The ground ice dynamics and ecological feedbacks greatly complicate efforts to assess permafrost responses to climate change.

1. Introduction

The vulnerability of permafrost to climate change depends on the complex interaction of climate, permafrost characteristics, and surface boundary conditions modified by ecological processes [Shur and Jorgenson, 2007; Grosse et al., 2011]. The extent to which permafrost terrain potentially can thaw and collapse is fundamentally controlled by the amount and type of ground ice [Danilov, 1990; Shur and Osterkamp, 2007; Pullman et al., 2007], leading to predictable patterns of thermokarst terrain [Jorgenson, 2013]. Once permafrost thaws everything about the system changes, however, creating ecological feedbacks that remain poorly understood [Jorgenson et al., 2010].

Ground ice morphology, abundance, and distribution in permafrost terrain are highly variable [French and Shur, 2010; Murton, 2013]. One of the most abundant forms of ground ice in the Arctic is ice wedges, because soil contraction and ice wedge polygon formation are common at mean annual air temperatures < -6°C. Ice wedges are abundant in Alaska [Péwé, 1963], Canada [Mackay, 1976], Russia [Dostovalov and Popov, 1963; Vtyurin, 1975; Romanovskii, 1985], and Svalbard [Christiansen, 2005]. In northern Alaska, wedge ice typically occupies 5-20% of the upper 3 m of permafrost, depending on surficial geology and age of deposit [Leffingwell, 1915; Kanevskiy et al., 2013; Jorgenson et al., 2014]. In extremely ice-rich eolian silt of Pleistocene age located along the lower foothills in northern Alaska, syngenetic ice wedges that formed concurrent with loess deposition occupy 30 to 70% of the volume of ~40 m thick yedoma deposits [Kanevskiy et al., 2011]. Ice wedges, which form just below the seasonally thawed active layer, are particularly vulnerable to climate change, and an abrupt increase in ice wedge degradation has occurred during the last two decades [Jorgenson et al., 2006; Raynolds et al., 2014]. Thermokarst cave ice, formed due to freezing of water in underground cavities created by thawing of a portion of the ice wedge, is frequently observed within

©2015. American Geophysical Union. All Rights Reserved.



and next to ice wedges [Mackay, 2000; Douglas et al., 2011; Kanevskiy et al., 2013]. In addition to massive ice, segregated ice typically forms an ice-rich intermediate layer in the upper permafrost in response to ecological succession and active layer adjustments, with pore and segregated ice occupying up to 90% of the soil volume [Shur, 1988; French and Shur, 2010]. An ice-poor transient layer, which forms as a result of fluctuations in the active layer thickness due to varying annual summer conditions, helps to protect the intermediate layer and ice wedges from thawing [Shur et al., 2005]. These varying types of ground ice in the upper permafrost aggrade and degrade in response to changing surface conditions and can be used to interpret the history of permafrost and paleoecological conditions [Burn, 1997; French and Shur, 2010; Kanevskiy et al., 2011].

Ecosystems undergo a large reorganization of their topography, hydrology, soil, and vegetation when ice-rich permafrost thaws [Osterkamp et al., 2009; Jorgenson et al., 2013]. The surface changes create strong positive feedbacks associated with impounding water and negative feedbacks associated with vegetation changes and organic matter accumulation that affect surface thermal regimes and permafrost stability [Jorgenson et al., 2006, 2010]. Initially, the positive feedbacks accelerate permafrost degradation, but ecological responses can quickly act to stabilize the surface and allow ground ice to reaggrade. Thus, continuous permafrost in cold climates can be characterized as climate-driven, ecosystem-modified permafrost [Shur and Jorgenson, 2007]. Permafrost thawing has large consequences for plant and wildlife habitats [Marcot et al., 2015], hydrology [Walvoord and Striegl, 2007; Liljedahl et al., 2012], energy balance [Gamon et al., 2012], soil carbon balance and trace gas emissions [McGuire et al., 2009; Sachs et al., 2010; Schuur et al., 2015], nutrient availability in adjacent waterbodies [Bowden et al., 2008; Kokelj et al., 2009; Koch et al., 2014], and land use and infrastructure [Arctic Research Commission Permafrost Task Force, 2003].

To assess the roles of ground ice and ecological feedbacks in ice wedge degradation and stabilization, we studied biophysical changes across a chronosequence of degradation and stabilization stages at Prudhoe Bay in northern Alaska during 2011–2014. Specific objectives of the research were to (1) evaluate ground ice dynamics by quantifying ice wedge volume, determining rates of ice wedge degradation through a time series of historical imagery, and characterizing ground ice types; (2) compare thermal regimes among stages; and (3) assess changes in and interactions among biophysical characteristics that provide positive and negative feedbacks that affect degradation and stabilization.

2. Methods

We conducted the research in wet tundra formed in an old, ice-rich, drained lake basin near Prudhoe Bay, Alaska [Walker et al., 1980]. The region has continuous permafrost because of low mean annual air temperatures (–11°C), and permafrost is approximately 600 m deep with abundant ice wedges [Kanevskiy et al., 2011]. While oilfield disturbances are prevalent in a gradient away from facilities [Raynolds et al., 2014], we considered the study area to be undisturbed because it was >500 m from the nearest active road, there was no evidence of surface dust accumulation or impoundments, and human-induced thermokarst typically occurs with 100 m of roads and facilities. Winter seismic trails were evident on the images from 1988 and 2009, but we considered their effects to be negligible because trails were not evident in subsequent years and there appeared to be no difference in thermokarst between trails and adjacent areas.

The study used a stratified, targeted sampling design to quantify biophysical changes associated with five stages of ice wedge degradation: undegraded (UD: narrow, well vegetated), degradation initial (DI: narrow with shallow flooding, abundant hydrophytic sedges, active layer encounters wedge ice), degradation advanced (DA: wide, deeply flooded), stabilization initial (SI: wide, shallowly flooded and sedge dominated), and stabilization advanced (SA: wide, above the water table, diverse vegetation, thick intermediate layer above wedge ice) with each stage replicated three time. For comparison with the degradation sequence, we also sampled three centers of ice wedge polygons (PC), two shallow (<1 m) lakes (LS) and one deep (~2 m) lake (LD). Most plots were established along a 350 m transect, but additional plots were established off transect when replicates of stages were not available along the transect (Figure 1 and supporting information Figure S1). At each intensive plot (three replicates for each stage), we sampled microtopography, water levels, snow depths, thermal parameters (soil temperatures, net radiation, and seasonal soil heat flux), soil stratigraphy, and vegetation cover. To assess ice wedge abundance, we did targeted coring across five wedges to quantify wedge dimensions and systematic coring at 10 m intervals along the transect. Initial instrumentation and soil coring was done in early June 2011, intensive sampling was done three times

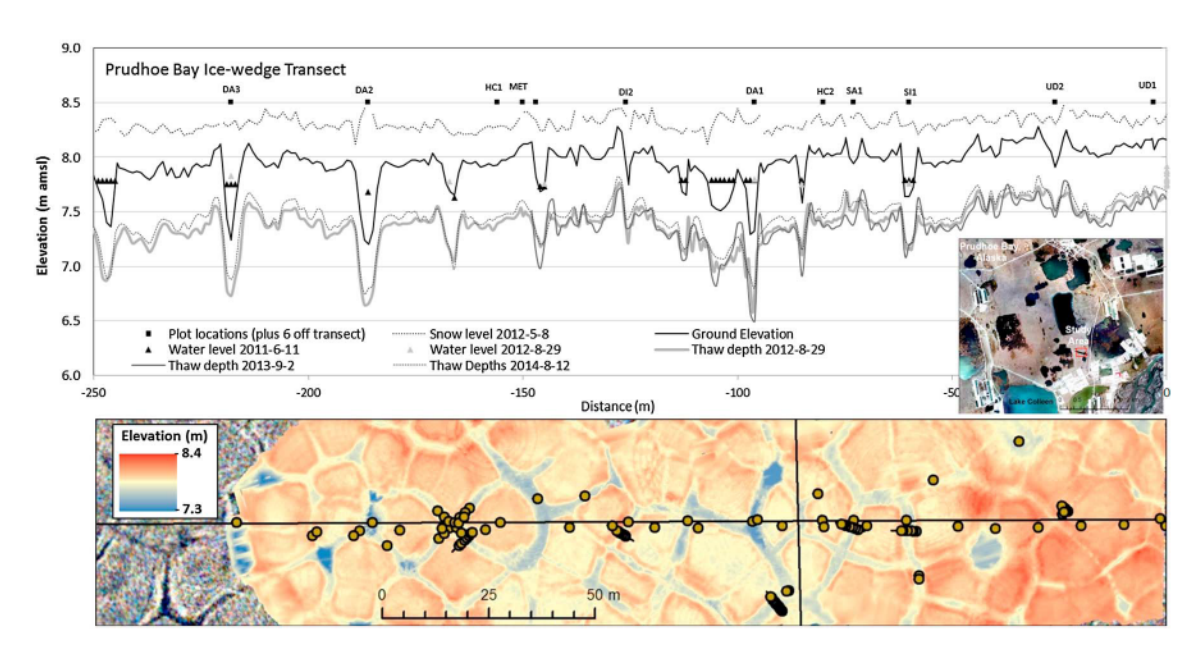


Figure 1. (top) Cross-sectional profile and (bottom) digital elevation model of the main sampling transect at Prudhoe Bay, Alaska (70.2288, -148.4186, 8.27 m amsl at T1-000). Plot locations, microtopography, thaw depths, water levels, and snow depth are shown.

(mid-June, late July, and late August) during summer 2012, and follow-up monitoring of microtopography, thaw depths, and soil temperatures was done in early September 2013 and 2014.

Thermokarst change over time was quantified by air photointerpretation of a time series of air photos (20 July 1949, 29 July 1968, 17 June 1977, 28 July 1982, 3 September 1988, 20 July 1997, 20 July 1997, 26 July 2004, and 14 July 2009) and high-resolution satellite imagery (6/15/12, Quickbird, color, 0.6 m resolution). Imagery was georectified to the orthorectified 2004 air photo. Waterbodies were manually delineated on each image, and thermokarst troughs (linear) were differentiated from waterbodies in polygon centers (round waterbodies within or crossing multiple polygon centers).

Ground ice volume for ice wedges was estimated using two methods. For the geometric method, ice volume was calculated as the average cross-sectional area of ice wedges times the average length of the ice wedge troughs mapped within three 1 ha areas. For the cross-sectional area, coring was done across five ice wedges and the dimensions of the wedges were interpolated from the occurrence of wedge ice in the cores. The widths of the wedges were then measured at 1 m depth increments from the top of the wedge from the interpolated scaled drawings (Figure 2). For each wedge, we calculated area for each 1 m increment (average of top and bottom widths x height) and summed the incremental volumes. We then averaged the cross-sectional areas for the five wedges sampled. For the cumulative length of ice wedges, we mapped the centerlines of ice wedge troughs evident on 2009 air photos (supporting information Figure S2). For the coring method, we did systematic coring at 10 m intervals along Transect 1 (offset 2 m south) to depths of 1.0 to 2.6 m. Because the coring was not to a consistent depth for all 21 cores, we made the following assumptions. First, if wedge ice was not encountered within 1–1.5 m (n = 10), we assumed no wedge ice was present to 3 m (typically in polygon centers). Second, for cores (n = 5) with deep wedge ice where we did not encounter the bottom contact of the wedge ice with soil, we calculated bottom depth based on wedge depth being a function of distance from wedge center (y = -1.54x + 2.88, $R^2 = 0.71$). Third, for cores (n = 5) where a contact with soil was found at the bottom of wedge ice we assumed all soil below the wedge ice to 3 m was free from additional wedge ice. Fourth, for one core where wedge ice was found, but the bottom was not determined, we used the measured length of wedge ice because the coring was sufficiently far (1.8 m) from the center of the wedge that additional ice should have been negligible. For each core, we then calculated the length and percent of wedge ice encountered within 1 m increments from the top of permafrost (below active layer and seasonal frost). We then calculated mean percent wedge ice for each 1 m increment across all cores.

Topography was quantified using leveling and ground-based lidar. Periodic measurements of ground surface elevations along the main transect were made using an autolevel and rod for centimeter level accuracy. For

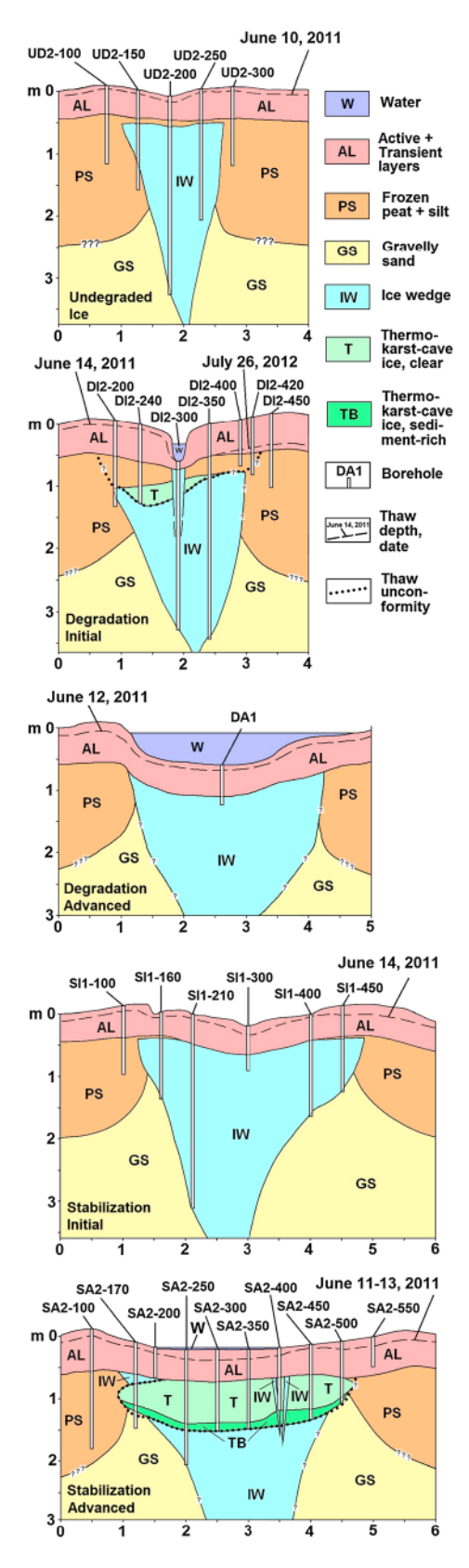


Figure 2. Cross-sections of ice wedges interpolated from cores. The sequence of degrading and stabilizing ice wedges illustrate differences in microtopography, soils, and ground ice characteristics.

the LIDAR measurements, we used a laser scanner (IS 3" Image Station, Topcon, Inc.) to measure surface elevations at ~1 million points. We estimate the accuracy to within 10 cm, given the occurrence of lowgrowing tundra vegetation. The Image Station was also used to measure coordinates (x, y, z) of the ground sediment surface of troughs and waterbodies using a A7R 360 Prism and Robotic Prism Pole. The surveys were referenced to a bench mark (BM) established at T1-000 (70.228815, 148.4186287, 8.27 m above mean sea level (amsl)), where coordinates were determined with a survey grade differential geographic positioning system (Topcon Hiper Lite+) and postprocessing.

Water and snow were measured periodically along the transect and at intensive plots and continuously at three DA plots. Water levels were measured with an autolevel on 14 June 2011, 11 June 2012, 26 July 2012, 29 August 2012, and 2 September 2013 in reference to the BM. For continuous water level measurements, we used pressure transducers (Hobo U20, Onset Corp.) to record water levels at 2 h intervals. We also measured water levels at T1-096 and T1-277 by using a time lapse camera to take pictures 3 times/day of staff gages established within the waterbodies. Snow was measured on 8 May 2012 with a ruler and snow density was measured with a coring tube and scale.

Soil temperatures were measured continuously at 18 intensive plots (three per stage), and microclimate parameters recorded at a single weather station. Soil temperatures were recorded every 2h using two-channel recorders (Hobo U23) with thermistor sensors near the surface (-5 cm) and permafrost table (50-60 cm). At several locations, four-channel dataloggers (Hobo Microstation) were used. The weather station used a Campbell datalogger (CR1000) to record air temperature, precipitation (RG3-m tipping bucket), ground temperatures (108-L sensor, at 2, 10, 20, 50, and 130 cm depths, hourly), and net radiation (NR-Lite2, every second, averaged to 10 min intervals). Periodic measurements (11 June, 22 July, and 26



August in 2012) of net radiation on cloud-free days also were made at each intensive site (1 m height) by recording data at 1 s intervals and averaging over a 3 min period. Net soil heat flux during the thaw season was calculated by summing the latent and specific heat contents in the active layer associated with thawing and heating the soil/water. This is only an approximation net flux into the soil/water because heat loss from the bottom of the active layer and potential thawing of thin layers of massive ice at the bottom of the active layer were not accounted for. We assumed the values to be small and vary little among sites. We used water and thaw depths, soil moisture contents, and temperatures collected on 26 August 2012. The latent heat for thawing ice of 334 MJ/m³, and specific heat capacities of 0.8 and 1.2 MJ/m³ per 1°C were used for the dry fractions of organic and organic mineral soils, respectively, and 4.19 MJ/m³ for water

Soil stratigraphy was described from 111 cores, and samples were taken from cores at the 18 intensive plots for physical and chemical analyses. In unfrozen surface soils, we extracted 30 cm diameter soil plugs of surface soils with a shovel for subsampling with knives or small corers. For frozen soils, we used a Snow, Ice, and Permafrost Research Establishment corer (7.5 cm diameter) and cored to 1–3.5 m depths. Soil stratigraphy was described according to U.S. Department of Agriculture-Natural Resources Conservation Service field sampling methods. Coarse fragment (>2 mm) percentage was visually estimated. Cryostructures were described according to *French and Shur* [2010]. Peat types were differentiated by dominant plant macrofossils identifiable in the field with a hand lens. Volumetric soil samples were obtained every ~20 cm with additional targeted samples taken from thin, distinctive horizons. In the field, determinations were made for wet weights, and soil pH and electrical conductivity were measured in thawed liquids or a saturated paste with a portable meter. Laboratory analyses for TCN and CaCO₃ were done by the Soil, Water and Plant Testing Laboratory, Colorado State University, Ft. Collins, CO.

Vegetation cover was sampled at the 18 intensive plots using a point intercept method. Plots were variable sizes (5 m long by 0.4, 1, or 2 m wide) to accommodate the varying width of the troughs. At 100 points per plot, the first occurrence of each species hit by a laser pointer was recorded. After point sampling, the plots were examined for additional species and a trace cover of 0.1% was assigned to species that were present but not captured in the point sampling. Voucher collections of unknown species were collected for later identification by specialists.

For data analysis, we compiled and aggregated the data into a simplified set of biophysical metrics appropriate for all degradation stages. We tested for effects of degradation stage on ecological parameters using the nonparametric Kruskal-Wallis analysis of variance. Plant composition differences among communities were analyzed with nonmetric multidimensional scaling (NMDS), a multivariate ordination technique, using PC-ORD 6.0 (MjM Software Design, Gleneden Beach, OR). The ordination axes represent the dominant patterns of species composition. Correlation analyses of the ordination axis scores with species and environmental data were conducted and presented as biplots, in which vector length and direction represent the strength and direction of the correlations. Data were assessed for normality and transformed prior to analysis. To evaluate ecological feedbacks, we used linear regression to quantify strength of relationships among biophysical factors. For assessing climatic effects on ice wedge degradation we obtained long-term weather data for the Kuparuk Station (USC00505136, 1983–2014), which has a longer and more complete record than Prudhoe Bay, from the National Climatic Data Center (http://www.ncdc.noaa.gov/), and thaw depth data from the Circumpolar Active Layer Monitoring (CALM) program [Nelson et al., 2008] from the CALM website (data available at http://www.gwu.edu/~calm/). Annual thaw degree days for Kuparuk were summarized from the mean daily temperatures.

3. Results

3.1. Ground Ice Volume and Dynamics

Ice wedge formation creates distinctive polygonal microtopography associated with low- and high-centered polygons, polygonal rims, and troughs (Figure 1). Mean ice wedge volume in the upper 3 m of permafrost (as % of layer volume) in our study area at Prudhoe Bay was $21.5 \pm 6.3\%$ (\pm SD), calculated from their average cumulative length of 1406 ± 39 m/ha determined from air photos and a cross-sectional area of 5.1 ± 1.5 m² determined from coring five wedges. Ice wedge dimensions were highly variable with an average width of 3.0 ± 1.0 m at the top and height of 3.3 ± 0.2 m (Figure 2). Mean ice wedge volume was $32.5 \pm 3.5\%$ for the top 1 m, $27.0 \pm 4.0\%$ for the top 2 m, $21.5 \pm 6.3\%$ for the top 3 m, and $16.3 \pm 4.9\%$ for

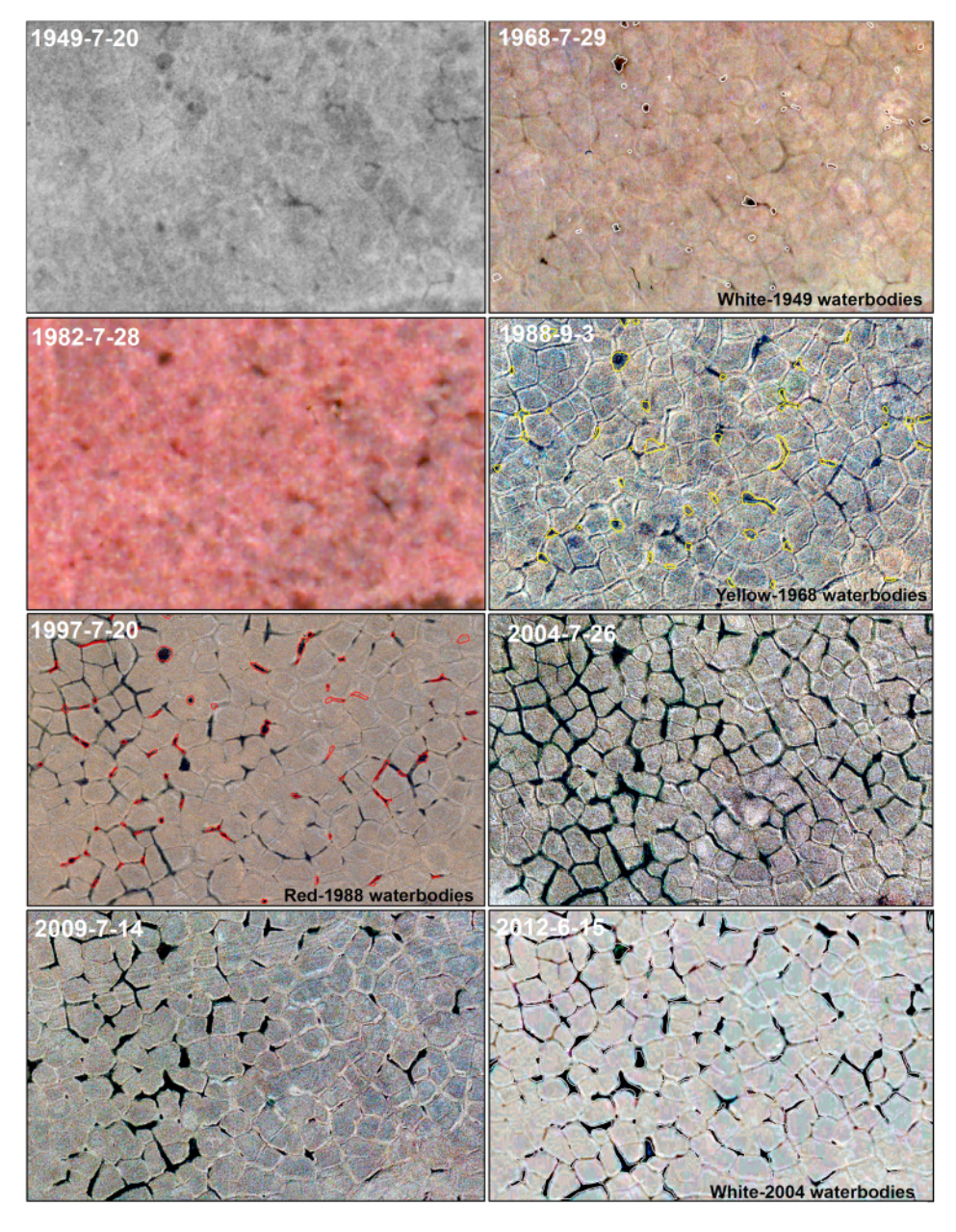


Figure 3. Changes in waterbody distribution associated with thermokarst troughs and low-centered polygons from 1949 to 2012 at Prudhoe Bay, Alaska. Waterbodies from previous years are overlaid on air photos.

the top 4 m of permafrost based on the geometry method. Mean wedge volumes by depth determined from the 21 systematically distributed cores were 31.1%, 27.5%, 18.0%, and 16.5%, respectively. Photographs of exposed ice wedges from other localities are provided in supporting information Figure S3.

Ice wedge degradation, as indicated by water-filled troughs that were evident on a time series of eight images from 1949 to 2012, showed a large increase in areal extent within the 6.7 ha study area during the last two decades (Figure 3). Thermokarst extent was relatively small from 1949 (0.9%) to 1988 (1.5%), abruptly increased from 1988 to 2004 (6.3%), and increased slightly from 2004 to 2012 (7.5%). Given that ice wedges occupy 32% of the upper 1 m of permafrost in the study area based on the geometric method, we estimate that ~23% (7.5%/32%) of the surface of the ice wedges has been degraded, but the degradation was usually limited to the top ~0.5 m of the wedges. Thermokarst troughs, with their deeper bottoms, also helped in redistributing water from polygon centers to troughs: extent of distinct waterbodies in polygon centers

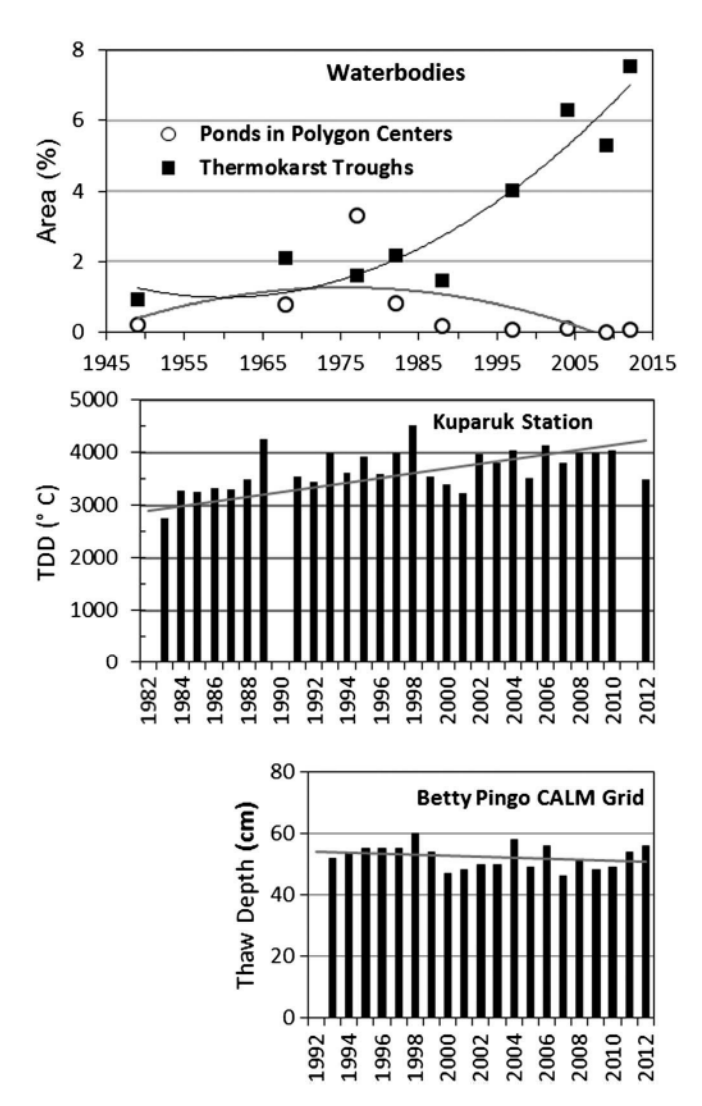


Figure 4. Summary of area extent of waterbodies in (top) study area, (middle) summer air temperatures expressed as thawing degree days (TDD) at Kuparuk Station, and (bottom) mean thaw depths at the Circumpolar Active Layer Monitoring site at Betty Pingo in Prudhoe Bay oilfield. Trendline is a second-order polynomial for waterbodies and linear for TDD and thaw depths.

varied from 0.2% in 1949 to 3.3% in 1977 and decreased to ≤0.1% by 1997. The image analysis, however, was sensitive to small changes in waterbody size as related to seasonality (early versus late summer), precipitation (wet versus dry year) and image quality (ability to resolve water/land boundary). For example, we attribute the changes water in thermokarst troughs from 2004 (6.3%) to 2009 (5.3%) seasonal/annual differences precipitation and not to reduction in thermokarst. Tracking of 212 waterbodies revealed periodic creation of thermokarst troughs: after 1949 (34 already present) most new waterbodies were created during 1989-2004 (80 over 15 years, 5.3/year), compared 1950–1982 (37 over 32 years, 1.1/year) and 2005-2012 (18 over 7 years, 2.3/year). Meanwhile, 19 disappeared, mostly by 1968.

We attribute the initial abrupt increase in ice wedge degradation to the extremely warm and wet summer of 1989 and subsequent thermokarst expansion to additional extremely warm summers of 1998 and 2004 (Figure 4). At the Kuparuk weather station (1983-2014), the two warmest summers on record based on thawing degree days (base 0°C) were 1989 (4261) and 1998 (4516), and both of these were followed by summers that were cooler than average (3698). Most of the 2000s were above average. When comparing periods before and after 1988, the degradation rate for the 1988-2004 period (0.30%/year) was 21

times higher than for the 1949–1988 period (0.01%/year). During the period (1993–2014) of recorded thaw depths at the Betty Pingo CALM site, mean thaw depths for the 1 km² grid also showed maximum thaw depths in 1998 and 2004, but the overall trend showed slightly decreasing, but highly variable, depths over time.

Five stages of degradation and stabilization were differentiated based on microtopography, surface water, vegetation, and ground ice characteristics (supporting information Figure S4) These include undegraded troughs (UD, narrow, well vegetated), degradation initial (DI, narrow with shallow flooding and abundant hydrophytic sedges), degradation advanced (DA, wide, deeply flooded), stabilization initial (SI, wide, shallowly flooded, sedge dominated), and stabilization advanced (SA, wide, above the water table, diverse vegetation). For comparison with this sequence, we also sampled the three undegraded centers of ice wedge polygons (PC), two shallow lakes (LS), and one deep lake (LD). We evaluated our initial classification of sites by analyzing the stratigraphy of soils cores at each site, resulting in reclassification of 2 of our 111 coring sites.

Ground ice underwent dynamic changes as permafrost degraded and stabilized (Figure 2). For simplicity, we combined the diverse types of cryostructures into five broad permafrost classes: (1) an ice-rich intermediate



layer (quasi-syngenetic permafrost with mostly ataxitic, reticulate, braided, and layered cryostructures); (2) epigenetic thermokarst cave ice (horizontally stratified massive ice) that forms in the thawed cavities of wedge ice; (3) epigenetic ice wedges (vertically foliated massive ice); (4) ice-poor transient layer (mostly lenticular, layered, vertical vein, and reticulate cryostructures) that is infrequently thawed due to fluctuations in active layer thickness; and (5) the ice-poor seasonally frozen active layer (mostly pore, lenticular, and organic matrix cryostructures). Overall mean depths (including active layer and frozen soil) to ice wedges where coring was sufficiently deep to encounter wedge ice (72 of 111 cores), were similar among early to middegradation stages (42.7–51.5 cm) but increased to 72.5 cm in SA (Figure 5). In UD, wedge ice occurred at a mean depth of 51.5 cm below the surface and was protected by a thick ice-poor transient layer and a thinner ice-rich intermediate layer (Figure 5). In DA, the protective layers were absent; wedge ice was in contact with the active layer, except where cave ice was evident in one of four cores. By the SA stage, there were substantial but highly variable thicknesses of cave ice (15.7 \pm 24.1 cm) and intermediate layer (13.5 \pm 19.6 cm), with only a thin transient layer (1.7 \pm 3.6 cm). Cave ice was found in 1 of 4 DA, 1 of 6 DI, 0 of 11 SI, and 22 of 46 SA cores. While we assigned stages to all sites, we note that some sites had transitional characteristics that did not classify neatly.

3.2. Thermal Regimes

Thermal regimes showed large differences in seasonal patterns of surface (–5 cm depth) and deep (–50 cm depth, near permafrost table) soil temperatures among degradation stages (Figure 6). Summer temperatures for surface soils were highest for DA and DI and lowest for SA and UD, while winter temperatures were coldest for UD and SA and warmest for DA. A nearby deep lake (LD), sampled in addition to the degradation stages, had the warmest summer soil (sediment surface) temperatures and the warmest winter temperatures, which did not go below freezing.

Mean annual surface temperatures (MAST) during 2012 (hydrologic year September 2011 to August 2012) showed significant differences (p < 0.05) among degradation stages (Figure 5) and were coldest for UD (-6.2° C), warmest in DA (-1.3° C), and intermediate for SI (-4.3° C) and SA (-5.5C). Across the full range of landscape conditions, MAST varied by 9.9°C from polygon centers (PC, -6.8° C) to the sediment surface temperatures of deep lakes (LD, 3.1° C). Mean annual deep temperatures had similar trends, ranging from -7.3° C for UD, to -3.5° C for DA, to -6.8° C for SA. Mean annual air temperature (1.5 m above ground) was -10.6° C.

Mean seasonal heat flux, approximated from latent and specific heat contents in the active layer and surface water, increased fourfold (p = 0.02) from 78 MJ/m² for UD to 321 MJ/m² for DA and back down to 125 MJ/m² for SA (Figure 5). These differences were associated with small differences in net radiation, as indicated by periodic measurements of net radiation during midday, clear sky conditions. Net radiation in mid-June varied significantly (p = 0.03) from $359 \pm 16 \, \text{W/m}^2$ for UD to $418 \pm 16 \, \text{W/m}^2$ for DA and then decreased to $364 \pm 22 \, \text{W/m}^2$ for SA. Continuous measurements of net radiation at one PC site showed net radiation was mostly positive during midsummer and became increasingly negative (soil losing heat) during late summer (supporting information Figure S4).

3.3. Ecological Feedbacks

Topographic, hydrologic, pedologic, and vegetative characteristics showed large differences among degradation stages (Figure 5). Ground surface elevations showed significant (p < 0.001) differences among stages, with mean elevations lower by 0.65 m in DA (7.27 m) compared to UD (7.92 m amsl) and then increasing by 0.5 m by the SA (7.77 m) stage.

Mean water levels at the end of summer 2011 varied significantly (p = 0.004) from -10.7 ± 5.4 cm (negative when below surface) for UD to 60 ± 2.4 cm for DA. Due to the lowered water levels in the troughs, water levels in PC were -15.0 ± 5.4 cm. Continuous monitoring of water levels in DA plots showed water levels to be highest in early summer at the end of snowmelt and at the end of summer before freezeup (Figure 7). Water levels dropped by 16-19 cm during midsummer evaporative drawdown. We attribute the late summer water rise to late summer rains, decreased evaporation, and drainage of water from adjacent polygon centers, which has been shown to be an important source of water to troughs in a similar setting [Koch et al., 2014]. Snow depths (Figures 1 and 5), which affect both winter thermal regimes and snowmelt input, also were significantly different (p < 0.001) among stages, with mean snow depths much deeper in DA (52.2 cm) compared to UD (31.8 cm).

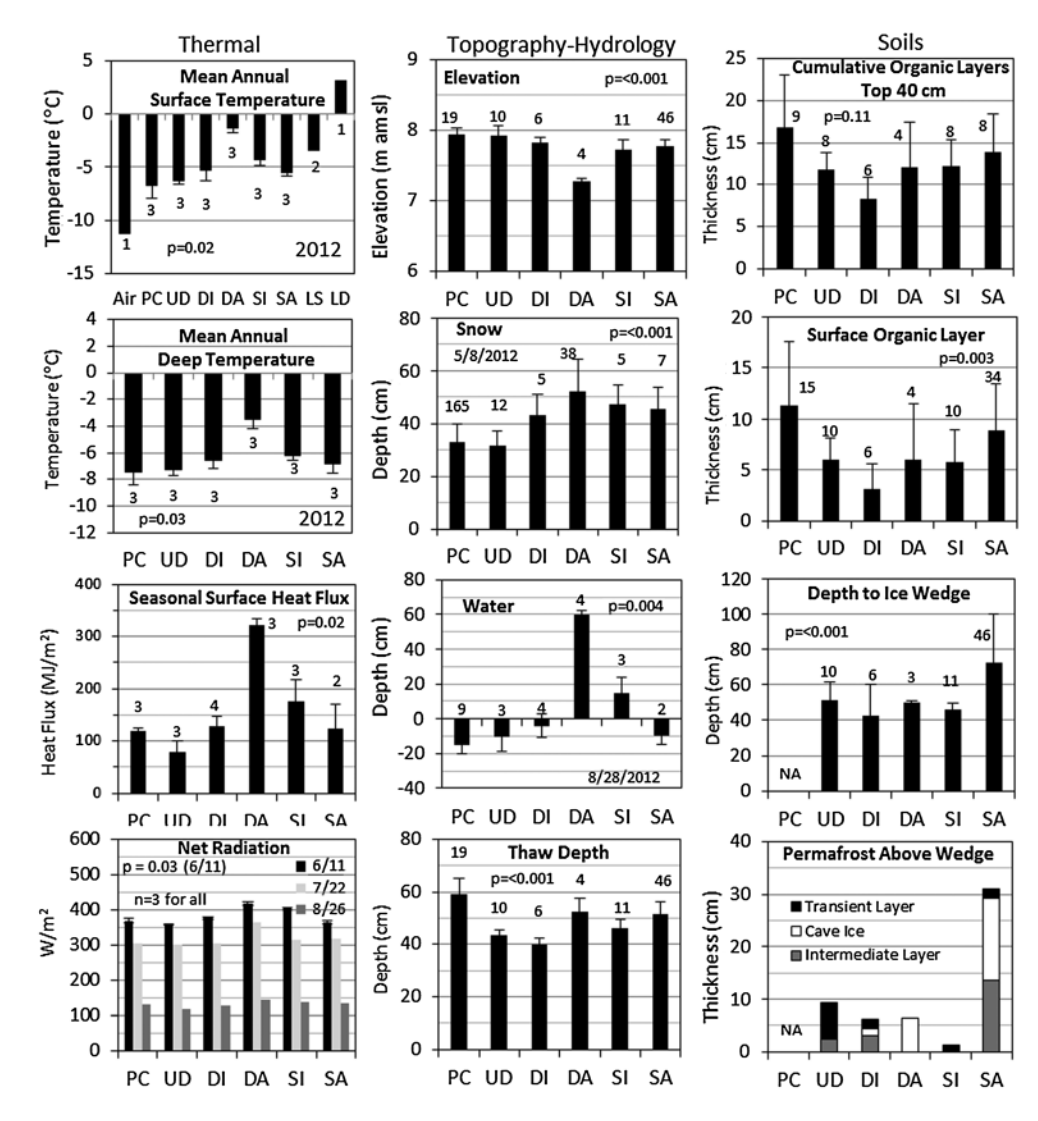


Figure 5. Mean (±SD) thermal (2012 only), topographic, hydrologic, and soil changes associated with degradation and stabilization of ice wedges. Stages include PC = polygon center, UD = undegraded wedges, DI = degradation initial, DA = degradation advanced, SI = stabilization initial, SA = stabilization advanced, air = air temperature, LS = lake shallow, and LD = lake deep. Provided above bars are sample sizes and overall significance (p) of treatment effects from Kruskal-Wallis one-way analysis of variance.

Soils above the ice wedges were frequently cryoturbated, with fibric and hemic organic masses intermixed with limnic organic-rich silts accumulated in a previous lacustrine environment. Slightly brackish and slightly pebbly loamy sands were commonly found at $1-3\,\mathrm{m}$ depth. Mean thickness of the surface organic layer varied threefold among stages, and SA had significantly (p=0.003) thicker organics than DI (Figure 5). Mean cumulative thickness within the top 40 cm had similar trends, but values were highly variable among stages and differences were not significant (p=0.11).

Mean thaw depths in late summer were significantly lower (p < 0.001) in UD (43.5 cm) and DI (39.7 cm) compared to DA (52.3 cm), SI (46.4 cm), SA (51.6 cm), and PC (59.0 cm). The difference in mean thaw depths and depths to ice wedges indicates how much frozen soil there was to protect wedge ice from seasonal thawing.

Vegetation cover underwent radical shifts in composition during ice wedge degradation and stabilization (Figure 8 and Table 1). The PC and UD sites were similar in that they had abundant dwarf shrubs (*Dryas integrifolia*, *Salix arctica*, and *Salix lanata*). The DI stage differed from other stages by having high cover of bare soil, intermediate cover of water, lack of dwarf shrubs, and high cover of sedges (*Eriophorum angustifolium* and *Carex bigelowii*).

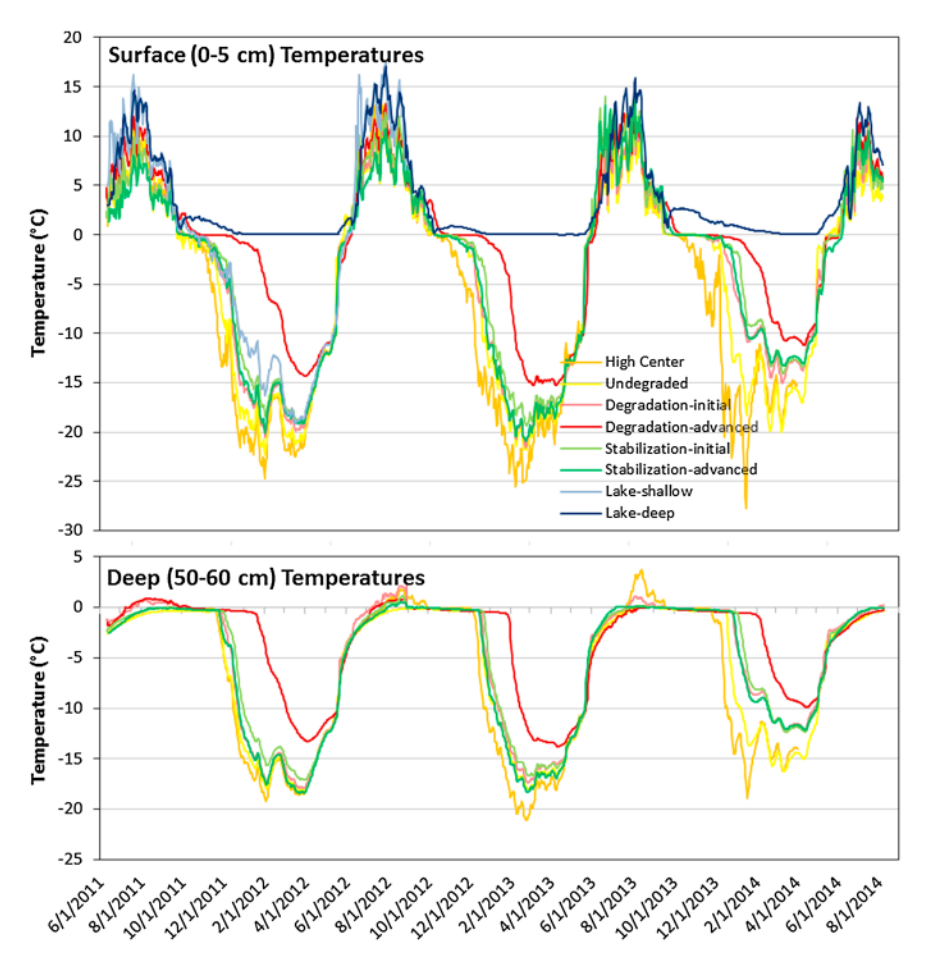


Figure 6. Mean daily surface and deep temperatures for five degradation stages, plus polygon center, shallow lake, and deep lake. Data are means for three sites per stage until 26 August 2012, thereafter only one site per stage.

The DA stage was dominated by calcareous aquatic mosses (Calliergon giganteum and Scorpodium scorpoides) and forbs (Utricularia vulgaris and Hippuris vulgaris). The SI stage was dominated by aquatic sedges (Carex aquatilis and E. angustifolium) and had a distinctive component of shallow hydrophytic mosses (Drepanocladus exannulatus and Drepanocladus revolvens) and grasses (Dupontia fisheri). SA was similar to UD with its minor component of dwarf shrubs but differed by the abundance of sedge Carex membranacea also found in SI but not other stages.

Interactions among these biophysical factors create strong ecological feedbacks on soil temperatures and permafrost stability. The NMDS analysis revealed species composition along Axis 1 was strongly positively related to both water depth (r=0.96) and mean annual surface temperature (r=.94) while negatively related to organic layer thickness (r=-0.38) (Figure 8). Thaw depths showed no relationship (r=-0.04) with the vegetation gradient along Axis 1. Regression analysis of biophysical factors revealed water depth was strongly related $(r^2=0.93)$ to differences in relative elevation caused by thawing ice wedges and surface collapse (Figure 9). Seasonal soil heat flux $(r^2=0.93)$ and MAST $(r^2=0.89)$ were strongly related to water depth. MAST was strongly affected by vascular plant cover $(r^2=0.94)$, Figure 8) but weakly affected by surface organic thickness $(r^2=0.08)$.

4. Discussion

4.1. Ground Ice Dynamics

Ice wedges fundamentally affect topography and soil properties in Arctic ecosystems. The ice wedge volume of 21% in the top 3 m of permafrost at our site was similar to the 12–16% in the upper 4.5 m reported for the

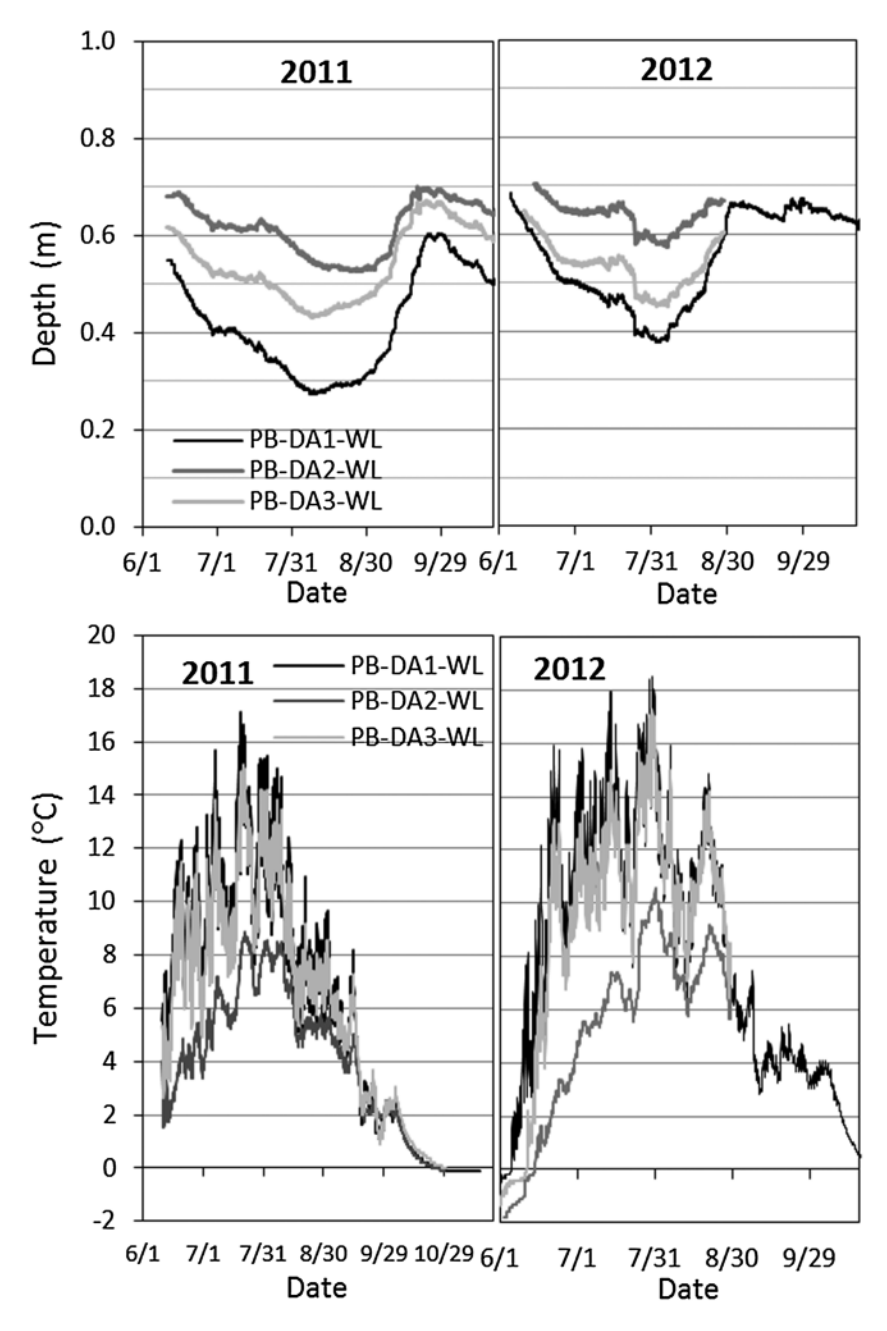


Figure 7. (top) Water levels and (bottom) temperatures in three thermokarst pits during summers 2011 and 2012 at Prudhoe Bay, Alaska.

Mackenzie Delta [Pollard and French, 1980], the 20% in the upper 2 m of abandoned floodplain deposits on the Colville Delta [Jorgenson et al., 1998], and the 14% for the upper 4 m for older terrain units in the western portion of the Beaufort Coastal Plain [Kanevskiy et al., 2013]. Within the top 1 m, however, ice volumes were much higher; 32% in our study because of ice volumes diminish rapidly with depth in relation to the shape of the ice wedges. Due to their high volume and formation just below the active layer with only a little protection from transient and intermediate permafrost layers, they are highly vulnerable to degradation from extreme seasonal weather conditions, long-term climate change, or disturbance. We attribute the recent onset of degradation to the extremely warm and wet summers in 1989 and 1998 (Figure 4). While we targeted our sampling at an area undergoing extensive degradation, we have observed similar increases in ice wedge degradation in our studies at Beaufort Lagoon, Jago River, Fish Creek, Itkillik River, and Barrow

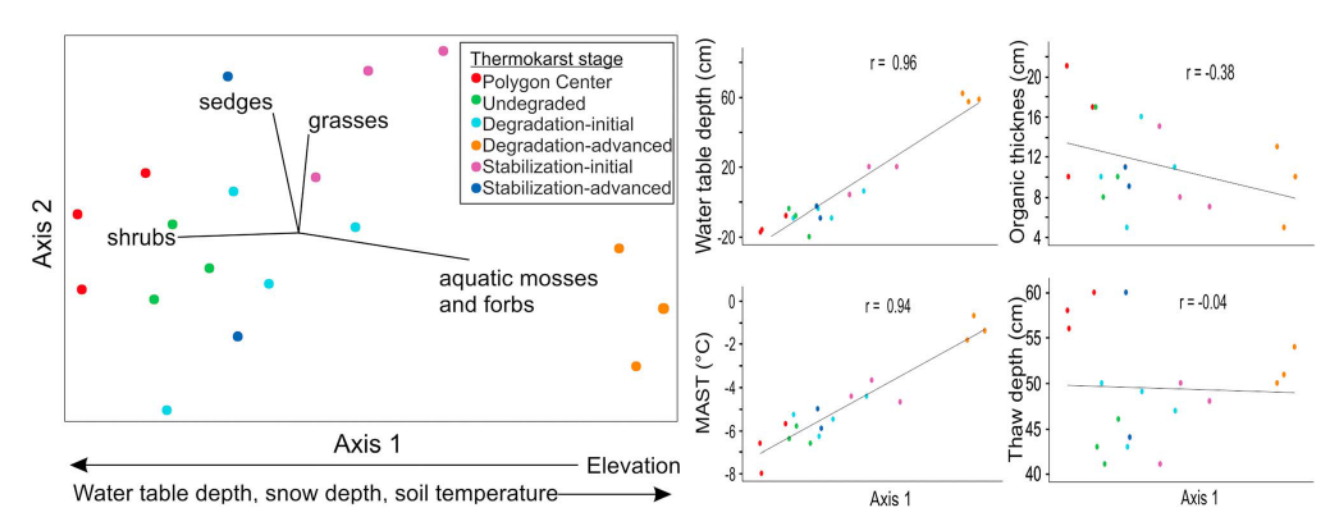


Figure 8. Ordination (nonmetric multidimensional scaling) of plots (colored by thermokarst stage) by plant species cover. Vectors show the direction and strength of significant correlations between plant groups and ordination axes ($r^2 \ge 0.4$). Below the ordination, arrows depict the direction of linear relationships between environmental variables and Axis 1.

in northern Alaska. Lidar also has recently been used to quantify thermokarst pits along the central Beaufort Sea coast [Jones et al., 2013]. Based on interpretation of air photos systematically distributed across Alaska, thermokarst troughs associated with ice wedge degradation covered 2.3% of northern Alaska in 2005 [Jorgenson et al., 2008]. Across the Arctic, substantial ice wedge degradation also has been observed in Canada [Fortier et al., 2007; Steedman, 2014] and Siberia [Fedorov et al., 2012; Helbig et al., 2013], indicating the degradation is widespread and having large effects on Arctic ecosystems.

The distribution of ground ice can be extremely variable, however, and is typically estimated by its relationship with landform soils, topography, and vegetation [Kreig, 1977; Kanevskiy et al., 2013; Jorgenson et al., 2014]. Determination of ice wedge volume is particularly problematic because variation occurs at the scale of meters. While our systematic coring confirmed that polygonal microtopography can be effective in estimating ice wedge volume in younger landscapes (late to mid-Holocene), in older landscapes (early Holocene and late Pleistocene) surface polygonalization is often obscured by soil and slope process. In older landscapes, we have frequently observed ice wedges within polygon centers that we attribute to earlier generations of ice wedge development (supporting information Figure S2). At our Prudhoe Bay site, some of the variation in wedge dimensions also may be related to the age of ice wedges developed through sequential subdivision of older large polygons with larger ice wedges into younger smaller polygons with smaller wedges in the younger subdivisions, as described by Mackay [1990]. Lack of adequate estimates of abundance and distribution of ground ice is one of the largest impediments to assessing ecological effects of permafrost degradation [Gogineni et al., 2014].

These results confirm that ground ice, by variations in type and distribution, not only controls the patterns and processes involved in the diverse modes of permafrost degradation [Jorgenson et al., 2008, 2013] but also affects stabilization processes. We summarize these processes in a conceptual model of ice wedge dynamics (Figure 10). New ice wedges develop on newly stabilized surfaces, such as floodplains and drained lake basins, over thousands of years (Mackay, 1976; Mackay, 1995; Harry and Gozdzik, 1988; Jorgenson et al., 1998; de Klerk et al., 2011). During initial degradation caused by extreme weather or disturbance, deepening of the active layer to contact and thaw underlying ice wedges leads to differential thaw settlement. Further collapse to the advanced degradation stage is facilitated by water impoundment and energy balance changes. The colonization of thermokarst troughs and pits by aquatic vegetation helps stall the degradation. During stabilization, ice aggrades in response to decreases in active layer thickness associated with vegetation changes, surface organic matter accumulation, and drainage changes, which leads to formation of a new intermediate layer [Shur et al., 2014]. The accumulating ice raises the surface, allowing better drainage toward adjacent low points. With the newly developed, thicker intermediate layer, the remnant ice wedges are more resilient to future degradation. In our undisturbed study area, ice wedges stabilized after only modest degradation, whereas anthropogenic disturbance has led to more severe degradation [Raynolds et al., 2014].



Life Form	Species	Polygon Center	Undegraded	Degraded Initial	Degraded Advanced	Stabilization Initial	Stabilization Advanced
Ch. I	•						
Shrub	Dryas integrifolia Salix arctica	5.7 12.7	10.0 4.7	1.3 0.1		0.1 1.0	0.1 1.0
						1.0	
	Salix lanata	3.0	1.4	1.0			0.1
	Salix ovalifolia	0.1	2.7	0.1		0.1	0.1
F. 1	Salix reticulata	0.1	2.7	0.1		0.1	0.1
Forb	Chrysantemum arcticum	0.1					0.1
	Draba sp.	0.1		0.1			0.1
	Equisetum variegatum	2.4	2.0	1.5		0.1	0.1
	Hippuris vulgaris				0.1		
	Melandrium apetalum	0.1		0.1			1.0
	Pedicularis lanata	0.1					0.1
	Pedicularis sudetica	0.1	0.1	0.1			
	Polygonum viviparum	1.7	1.4	0.1		0.1	2.0
	Saxifraga hirculus	0.1	0.1				1.5
	Saxifraga oppositifolia	0.1	0.1	0.1			
	Senecio atropurpureus		0.1				
	Utricularia vulgaris				17.7		
Grass/	Dupontia fisheri					0.1	
Sedge	Carex aquatilis			0.1	4.0	13.3	1,1
	Carex atrofusca	2.0	2.0	0.1			0.1
	Carex bigelowii	4.3	8.3	8.5		5.7	2.0
	Carex membranacea			0.1		1.4	6.0
	Carex misandra	4.3					
	Carex rotundata			0.1			
	Eriophorum angustifolium	0.1	10.3	12.8	0.1	13.0	25.5
	Eriophorum scheuchzeri			0.1		0.1	
	Eriophorum triste	7.7					
Moss	Aulacomnium palustre		0.1				
	Brachythecium cirrosum	1.0	0.1				0.1
	Bryoerythrophyllum rubrum	0.1		0.1			
	Bryum pseudotriquetrum		0.1				
	Calliergon giganteum			0.1	14.7	1.0	
	Calliergon richardsonii			0.1			
	Campylium stellatum	1.1	2.7	0.1		4.0	1.0
	Catoscopium nigritum	2.0	1.0	0.1			3.0
	Cinclidium latifolium			0.1		0.1	0.1
	Ctenidium molluscum			1.0			
	Dicranum elongatum	0.1	0.1				
	Distichium capillaceum	0.1	0.1	0.1			0.1
	Ditrichum flexicaule		0.1	0.1			0.1
	Drepanocladus	3.3	1.7	4.3		3.3	0.1
	exannulatus						
	Drepanocladus revolvens	2.7				2.7	
	Drepanocladus uncinatus	1.7	4.0	1.3			
	Meesia triquetra			2.0		0.1	
	Meesia uliginosa					1.0	
	Orthothecium chryseum		0.1	0.1			0.1
	Pseudocalliergon brevifolius	0.1	0.1				
	Pseudocalliergon turgescens	0.1	0.1	0.1		0.1	0.1
	Scorpidium cossonii	0.1		0.1		0.1	
	Scorpodium revolvens						0.1
	Scorpodium scorpoides			0.1	10.7		
	Tomenthypnum nitens		4.7	0.1	- 3		
	Tortella fragillis		0.1	0.1			
Lichen	Cetraria cucullata						0.1
	Stereodon bambergeri		0.1				0.1
	Thamnolia vermicularis			0.1			0.1

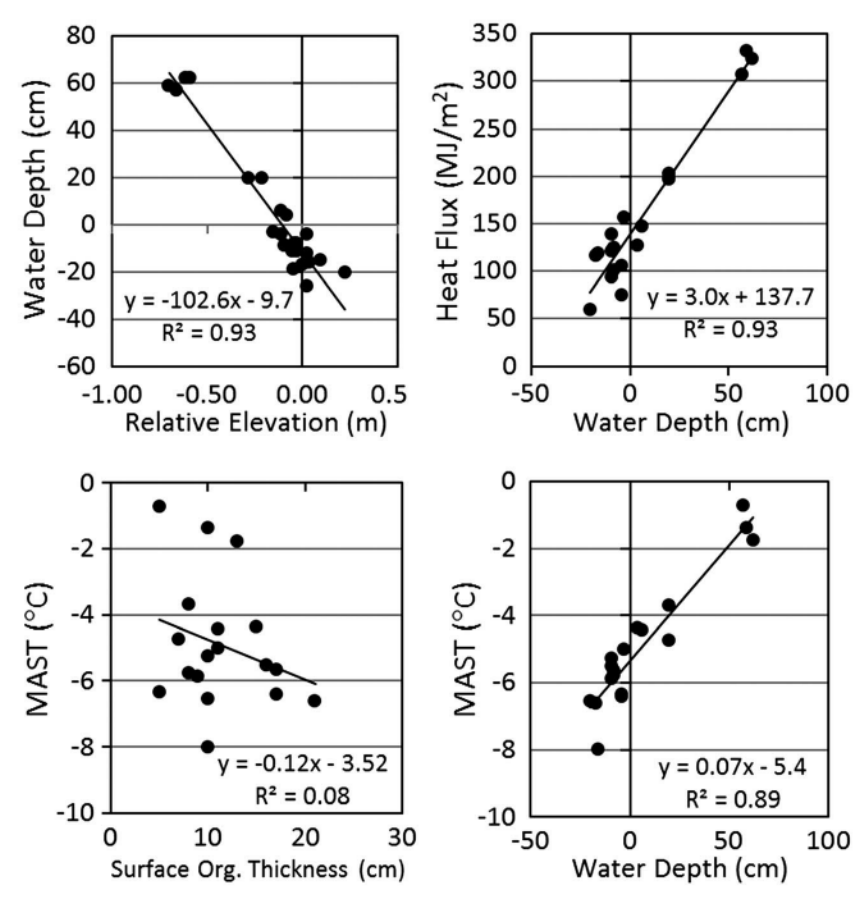


Figure 9. Relationships among biophysical factors providing feedbacks that affect permafrost stability. MAST = mean annual surface temperature, data from intensive plots in all degradation stages.

While we do not have sufficient data to adequately assess the period required for degradation and stabilization, field observations and the air photo analysis indicate after the long period of ice wedge formation (thousands of years for large wedges) nearly complete degradation can occur within a decade. Initial stabilization can occur within another decade and that it may take 30–100 years to achieve advanced stabilization (we observed only a few locations that had transitioned from DA to SA on the air photo time series).

Ice wedge dynamics can involve other pathways, depending on ice volumes and surface responses. Early stabilization can occur if surface water is redistributed, such as from troughs to deeper pits that develop at ice wedge intersections, that allows the surface to become better drained. Deep lakes can occur if ice wedges occupy sufficient volume (presumably >40%) and degrade completely. While ice wedge changes can be important to lake development [Billings and Peterson, 1980; Grosse et al., 2012], complete degradation to a thermokarst lake has a low probability [Shur and Osterkamp, 2007]. Theoretically, a thaw-lake cycle can occur when drainage of a thermokarst lake exposes a new surface that allows new ice wedge aggradation [Billings and Peterson, 1980], but the processes are sufficiently slow, and other geomorphic processes and climate changes typically intervene, so that a complete cycle is uncommon [Jorgenson and Shur, 2007]. Secondary wedge development can occur within an older wedge after advanced stabilization (see supporting information Figure S3c), often with thermokarst cave ice present as evidence of earlier degradation.

Ground ice also complicates the monitoring of permafrost stability. Thaw depths showed an inconsistent trend among degradation and stabilization stages, with mean thaw depths in DA being only slightly deeper that UD and DI and similar to SI and SA (Figure 5). Similarly, there was a lack of a long-term trend in mean thaw depths across the broader landscape near the Betty Pingo CALM site during a time of climate warming (Figure 4). Together, the results indicate thaw depth measurements alone are a poor indicator of permafrost stability in regions with cold, continuous permafrost and that surface subsidence measurements are needed

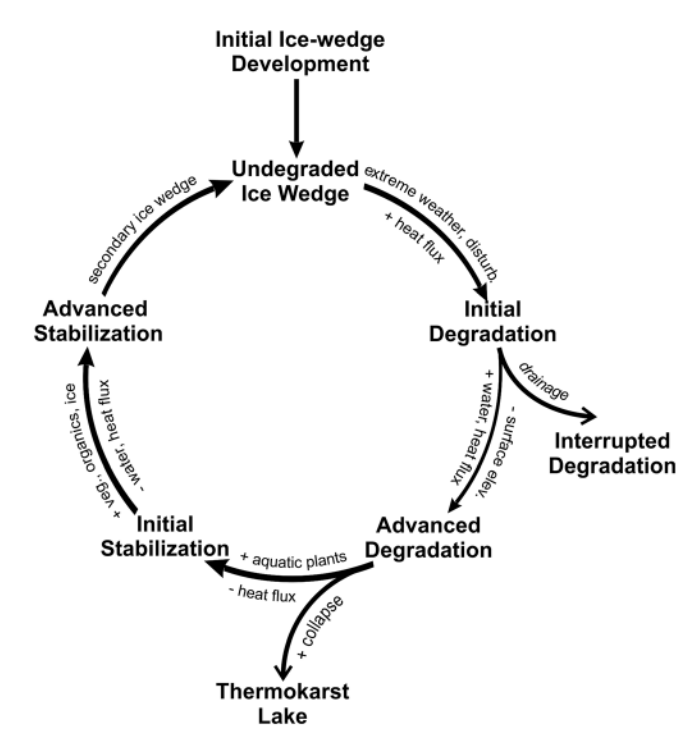


Figure 10. Conceptual model of cyclic ice wedge degradation and stabilization. Main stages are shown in bold, while biophysical factors affecting transitions are shown along arrows. Positive feedbacks with increasing heat flux are on the right, while negative feedbacks with decreasing heat flux are on the left. See Figure 2 for graphic illustrations of the stages.

[Jorgenson et al., 2006; Shiklomanov et al., 2013], because the presence of ice-rich permafrost below the active layer allows thawing to occur with little accumulation of additional soil in the active layer [Pullman et al., 2007].

4.2. Ecological Feedbacks

Once degradation is initiated by extreme seasonal weather, ecological feedbacks strongly control the degradation and stabilization process. Surface water provides a strong positive feedback, where thaw settlement creates deeper depressions and impounds more water, eventually leading to nearly a tripling of seasonal heat flux and a MAST increase of ~5°C. If degradation continues and forms a thermokarst lake, where mean annual temperatures at the sediment surface rise above 0°C, a thick unfrozen layer (closed talik) can development even under very cold climatic conditions.

Immediately upon thaw, plant growth dominated by aquatic mosses and sedges initiates negative feedbacks that stabilize the surface by reducing net

radiation input and convective heat transfer to surface sediments. Plant composition and growth is strongly controlled by microsite characteristics [Minke et al., 2009] and can be stimulated by the nutrients released by disturbance [Bowden et al., 2008; Koch et al., 2014] or soil warming [Euskirchen et al., 2009]. Slumping of materials from the banks of the troughs may contribute to stabilization by adding soil at the bottom of the pits and thickening the protective layers. In some cases, initial freeze back and stabilization can be rapid as evidenced by the frequent occurrence of thermokarst cave ice. Continued vegetation growth and compositional shifts, organic matter accumulation in saturated soils, and ice aggradation and heaving causes the surface to become better drained and lessen the radiative effects of surface water.

The ice wedge degradation has occurred even though mean annual air temperatures in northern Alaska have remained below -10°C, indicating that both ground ice and ecological feedbacks play a central role in degradation once initiated by extreme weather or climate change. The onset of rapid ice wedge degradation has occurred coincident with the decline in sea ice. The decline in sea ice, as well as snow cover, has accelerated since the 1990s, playing a central role in the amplification of Arctic air temperatures, with consequences for growing season length and tundra greenness [Screen and Simmonds, 2010; Bhatt et al., 2010; Post et al., 2013], as well as permafrost degradation near the coast [Günther et al., 2015].

4.3. Implications of Ice Wedge Degradation

Climate warming is projected to severely reduce permafrost distribution by the end of this century [Marchenko et al., 2008; Jafarov et al., 2012], but our results indicate permafrost responses will be greatly complicated by the ground ice dynamics and ecological feedbacks. The strengths of the feedbacks cause surface temperature changes that are double those of projected air temperature increases. Ground temperatures varied by 4.9°C (MAST) across the degradation and stabilization stages and by 9.9°C across the broader landscape from polygon centers to deep lakes. The temperature range is as large as the ~10°C range in mean annual air temperatures across the continuous to sporadic permafrost zones in Alaska [Jorgenson et al., 2008] and nearly double the projected warming for northern Alaska by the end of the century under an intermediate (A1B) greenhouse gas emission scenario [Scenarios-Network-for-Arctic-Planning, 2014].



The radical ecological changes and strong feedbacks make it very difficult to model the effects of permafrost degradation, especially at regional to global scales. Currently, these factors are absent in permafrost thermal models, dynamic ecosystem models, and global climate models used to project future permafrost distribution, soil carbon balance, and ecosystem distribution. While some modelers are cognizant of these processes, they are difficult to implement because of the lack of information on ground ice distribution, challenges in developing numerical models that can handle a collapsing surface that alters vertical layers (water, ice, and soil) and lateral hydrologic flow, and uncertainty in changes in both vegetation structure and composition. Furthermore, the microscale changes make it difficult to scale up to the kilometer resolution of regional models.

Permafrost degradation is a global concern because the amounts of soil organic carbon sequestered in frozen soils are much larger that the pool of atmospheric carbon, so decomposition of even a small fraction of this carbon and release of radiatively active trace gasses can have potential positive feedbacks to the climate system [McGuire et al., 2009; Schuur et al., 2015]. Once ice-rich permafrost thaws, however, all components of the ecosystem radically reorganize [Jorgenson et al., 2013], leading to changing wetting and drying soil conditions, changing primary productivity, and species composition that makes assessment of the soil carbon balance difficult [Schuur et al., 2015]. In cold permafrost terrain with ice wedge polygons, microsite variations in topography and moisture strongly affected methane emissions [Sachs et al., 2010]. At our site, ice wedge degradation led to flooded anaerobic soil conditions in troughs that potentially could enhance methane production and better drained aerobic soils in high-centered polygons that could enhance soil decomposition and carbon dioxide emissions. These results point to the need to better monitor ecological and landform changes, especially in areas with ice-rich permafrost that have landforms, such as ice wedge polygons, indicative of ground ice conditions. This will enable improved understanding of the rates of thermokarst, and the ground ice dynamics and ecological feedbacks that affect those rates, that can be incorporated into future projections of permafrost degradation and soil carbon dynamics.

5. Conclusion

After an initial increase in seasonal thawing in response to unusually warm and wet summers, ground ice dynamics and ecological feedbacks strongly control the degradation and stabilization of ice wedges. Thaw settlement along the polygonal networks of ice wedges causes increased water impoundment, soil heat flux, and soil temperatures that provide positive feedbacks that reinforce thawing and collapse. The disturbance, however, stimulates the growth of aquatic moss and herbaceous plant and the accumulation of surface organic matter that lead to decreased thaw depths, aggradation of new ground ice, heaving of the surface, reduction in surface water, and lower soil temperatures that stabilize the surface. These feedbacks, which cause mean annual soil surface temperatures to vary by 10°C across the landscape, are stronger than the projected effects of warming air temperatures alone and greatly complicate efforts to model and predict the impacts of climate warming on permafrost stability.

Acknowledgments

The data are available from the authors upon request and will be available on the National Science Foundation ACADIS gateway (https://www.aoncadis. org/home.htm). The research was funded by NSF grant ARC 1023623, and logistical support was provided by CH2MHill Polar Services. The U.S. Geological Survey provided additional financial support. Katie Nicolato, Doug Halm, Travis Drake, and Karen Jorgenson helped with field sampling. We appreciate the long-term data set of thaw depths provided by the CALM project.

References

Arctic Research Commission Permafrost Task Force (2003), Climate change, permafrost, and impacts on civil infrastructure, Spec. Rep. 01-03, U.S. Arctic Research Commission, Arlington, Va. 62 p.

Bhatt, U. S., D. A. Walker, M. K. Raynolds, J. C. Comiso, H. E. Epstein, G. Jia, R. Gens, C. E. Tweedie, C. J. Tucker, and P. J. Webber (2010), Circumpolar Arctic tundra vegetation change is linked to sea ice decline, Earth Interact., 14(8), 1-20, doi:10.1175/2010El315.1.

Billings, W. D., and K. M. Peterson (1980), Vegetational change and ice-wedge polygons through the thaw lake cycle in Arctic Alaska, Arctic

Bowden, W. B., M. N. Gooseff, A. Balser, A. Green, B. J. Peterson, and J. Bradford (2008), Sediment and nutrient delivery from thermokarst features in the foothills of the North Slope, Alaska: Potential impacts on headwater stream ecosystems, J. Geophys. Res., 113, G02026,

Burn, C. R. (1997), Cryostratigraphy, paleogeography, and climate change during the early Holocene warm interval, western Arctic coast, Canada, Can. J. Earth Sci., 34(7), 912-925, doi:10.1139/e17-076.

Christiansen, H. H. (2005), Thermal regime of ice-wedge cracking in Adventdalen, Svalbard, Permafrost Periglac. Proc., 16(1), 87-98, doi:10.1002/ppp.523.

Danilov, I. D. (1990), Underground Ice (in Russian), Nedra, Moskow.

de Klerk, P., N. Donner, N. S. Karpov, M. Minke, and H. Joosten (2011), Short-term dynamics of a low-centred ice-wedge polygon near Chokurdakh (NE Yakutia, NE Siberia) and climate change during the last ca 1250 years, Quat. Sci. Rev., 30(21-22), 3013-3031, doi:10.1016/i.guascirev.2011.06.016.

Dostovalov, B. N., and A. I. Popov (1963), Polygonal systems of ice-wedges and conditions of their development, in Proceedings International Conference on Permafrost, edited by K. B. Woods, pp. 102-105, Natl. Acd. of Sci., Natl. Res. Council, Washington, D. C.

Douglas, T. A., D. Fortier, Y. Shur, M. Kanevskiy, L. Guo, Y. Cai, and M. Bray (2011), Biogeochemical and geocryological characteristics of wedge and thermokarst-cave ice in the CRREL permafrost tunnel, Alaska, Permafrost Periglac. Proc., 22(2), 120-128, doi:10.1002/ppp.709.



- Euskirchen, E. S., A. D. McGuire, F. S. Chapin III, and S. Yi (2009), Changes in plant communities in northern Alaska under scenarios of climate change 2003-2100: Implications for climate feedbacks, Ecol. Appl., 19(4), 1022-1043, doi:10.1890/08-0806.1.
- Fedorov, A. N., P. P. Gavriliev, P. Y. Konstantinov, T. Hiyama, Y. lijima, and Y. Iwahana (2012), Contribution of thawing permafrost and ground Ice to the water balance of young thermokarst lakes in central Yakutia, in Proceedings of the Tenth International Conference on Permafrost, edited by K. Hinkel, pp. 75-80, The Northern Publisher, Tyumen, Russia.
- Fortier, D., M. Allard, and Y. Shur (2007), Observation of rapid drainage system development by thermal erosion of ice wedges on Bylot Island, Canadian Arctic Archipelago, Permafrost Perialac, Proc., 18, 229-243, doi:10.1002/ppp.595.
- French, H. M., and Y. Shur (2010), The principles of cryostratigraphy, Earth Sci. Rev., 101, 190-206, doi:10.1016/j.earscirev.2010.04.002.
- Gamon, J. A., G. P. Kershaw, S. Williamson, and D. S. Hik (2012), Microtopographic patterns in an arctic baydjarakh field: do fine-grain patterns enforce landscape stability? Environ. Res. Lett., 7, 015502, doi:10.1088/1748-9326/7/1/015502.
- Gogineni, P., V. Romanovsky, J. Cherry, C. Duguay, S. Goetz, M. T. Jorgenson, and M. Moghaddami (2014), Opportunities to use Remote Sensing in Understanding Permafrost and Related Ecological Characteristics: Report of a Workshop, 97 pp., Natl. Acad. of Sci.,
- Grosse, G., V. Romanovsky, T. Jorgenson, K. W. Anthony, and J. Brown (2011), Vulnerability and feedbacks of permafrost to climate change, Eos Trans. AGU, 92, 73-80.
- Grosse, G., B. Jones, and C. Arp (2012), Thermokarst lakes, drainage, and drained basins, in Treatise on Geomorphology, edited by J. F. Shroder, pp. 325-353, Academic Press, San Diego, Calif.
- Günther, F., P. P. Overduin, I. A. Yakshina, T. Opel, A. V. Baranskaya, and M. N. Grigoriev (2015), Observing Muostakh disappear: permafrost thaw subsidence and erosion of a ground-ice-rich island in response to arctic summer warming and sea ice reduction, Cryosphere, 9(1), 151-178, doi:10.5194/tc-9-151-2015.
- Harry, D. G., and J. S. Gozdzik (1988), Ice wedges: Growth, thaw transformation, and palaeoenvironmental significance, J. Quat. Sci., 3, 39-55, doi:10.1002/jqs.3390030107.
- Helbig, M., J. Boike, M. Langer, P. Schreiber, B. R. Runkle, and L. Kutzbach (2013), Spatial and seasonal variability of polygonal tundra water balance: Lena River Delta, northern Siberia (Russia), Hydrogeol. J., 21(1), 133-147, doi:10.1007/s10040-012-0933-4.
- Jafarov, E. E., S. S. Marchenko, and V. E. Romanovsky (2012), Numerical modeling of permafrost dynamics in Alaska using a high spatial resolution dataset, Cryosphere, 6, 613-624, doi:10.5194/tc-6-613-2012.
- Jones, B. M., J. M. Stoker, A. E. Gibbs, G. Grosse, V. E. Romanovsky, T. A. Douglas, N. E. M. Kinsman, and B. M. Richmond (2013), Quantifying landscape change in an arctic coastal lowland using repeat airborne LiDAR, Envinron. Res. Lett., 8, 045025, doi:10.1088/1748-9326/8/4/045025.
- Jorgenson, M. T. (2013), Thermokarst terrains, in Treatise on Geomorphology, edited by J. Schroeder, R. Giardino, and J. Harbor, pp. 313–324, Academic Press, San Diego, Calif.
- Jorgenson, M. T., and Y. Shur (2007), Evolution of lakes and basins in northern Alaska and discussion of the thaw lake cycle, J. Geophys. Res., 112, F02S17, doi:10.1029/2006JF000531,
- Jorgenson, M. T., Y. Shur, and H. J. Walker (1998), Factors affecting evolution of a permafrost dominated landscape on the Colville River Delta, northern Alaska, in Proceedings of Seventh International Permafrost Conference, edited by A. G. Lewkowicz and M. Allard, pp. 523-530, Universite Laval, Sainte-Foy, Quebec.
- Jorgenson, M. T., Y. L. Shur, and E. R. Pullman (2006), Abrupt increase in permafrost degradation in Arctic Alaska, Geophys. Res. Lett., 33, L02503, doi:10.1029/2005GL024960.
- Jorgenson, M. T., Y. L. Shur, and T. E. Osterkamp (2008), Thermokarst in Alaska, in Proceedings Ninth International Conference on Permafrost, edited by D. L. Kane and K. M. Hinkel, pp. 869-876, Inst. of Northern Engineering, Univ. of Alaska, Fairbanks, Alaska.
- Jorgenson, M. T., V. Romanovsky, J. Harden, Y. Shur, J. O'Donnell, E. A. G. Schuur, M. Kanevskiy, and S. Marchenko (2010), Resilience and vulnerability of permafrost to climate change, Can. J. For. Res., 40, 1219-1236, doi:10.1139/X10-060.
- Jorgenson, M. T., et al. (2013), Reorganization of vegetation, hydrology and soil carbon after permafrost degradation across heterogeneous boreal landscapes, Environ. Res. Lett., 8(035017), 13, doi:10.1088/1748-9326/8/3/035017.
- Jorgenson, M.T., M. Kanevskiy, Y. Shur, J. Grunblatt, C. L. Ping, and G. Michaelson (2014), Permafrost database development, characterization, and mapping for northern Alaska, Arctic Landscape Conservation Cooperative, Fairbanks, Alaska. [Available at http://www.gina.alaska. edu/projects/permafrost-database-and-maps-for-northem-alaska.]
- Kanevskiy, M. Z., Y. Shur, D. Fortier, M. T. Jorgenson, and E. Stephani (2011), Cryostratigraphy of late Pleistocene syngenetic permafrost (yedoma) in northern Alaska, Itkillik River exposure, Quat. Res., 75, 584-596, doi:10.1016/j.yqres.2010.12.003.
- Kanevskiy, M., Y. Shur, M. T. Jorgenson, C. L. Ping, G. J. Michaelson, D. Fortier, E. Stephani, M. Dillon, and V. E. Tumskoy (2013), Ground ice in the upper permafrost of the Beaufort Sea coast of Alaska, Cold Rea. Sci. Technol., 85, 56-70, doi:10.1016/j.coldregions.2012.08.002.
- Koch, J. C., K. Gumey, and M. S. Wipfli (2014), Morphology-dependent water budgets and nutrient fluxes in Arctic thaw ponds, Permafrost Perialac, Process., 25(2), 79-93, doi:10.1002/ppp.1804.
- Kokelj, S. V., B. Zajdlik, and M. S. Thompson (2009), The impacts of thawing permafrost on the chemistry of lakes across the subarctic borealtundra transition, Mackenzie Delta region, Canada, Permafrost Periglac. Proc., 20, 185-199, doi:10.1002/ppp.641.
- Kreig, R. A. (1977), Terrain analysis for the Trans-Alaska pipeline, Civil Eng. ASCE, 47(7), 61-65.
- Leffingwell, E. d. K. (1915), Ground-ice wedges, the dominant form of ground-ice on the north coast of Alaska, J. Geol., 23, 635-654.
- Liljedahl, A. K., L. D. Hinzman, and J. Schulla (2012), Ice-wedge polygon type controls low-gradient watershed-scale hydrology, in Tenth International Conference on Permafrost, edited by K. M. Hinkel, pp. 231-236, The Northern Publisher, Salekhard, Russia.
- Mackay, J. R. (1976), Ice-wedges as indicators of recent climatic change, western Arctic coast, Pap. 76-1A, pp. 233-234, Geol. Surv. of Canada.
- Mackay, J. R. (1990), Some observation on the growth and deformation of epigenetic, syngenetic and anti-syngenetic ice wedges, Permafrost Perialac. Proc., 1, 15–29, doi:10.1002/ppp.3430010104.
- Mackay, J. R. (1995), Ice wedges on hillslopes and landform evolution in the late Quaternary, western Arctic coast, Canada, Can. J. Earth Sci., 32(8), 1093-1105, doi:10.1139/e95-091.
- Mackay, J. R. (2000), Thermally induced movements in ice-wedge polygons, western Arctic coast: a long-term study, Geogr.Phys. Quatern., 54(1), 41-68, doi:10.7202/004846ar.
- Marchenko, S., V. Romanovsky, and G. Tipenko (2008), Numerical modeling of spatial permafrost dynamics in Alaska, in Proceedings of the Ninth International Conference on Permafrost, edited by D. L. Kane and K. M. Hinkel, pp. 1125-1130, Inst. of Northern Engineering, Univ. of Alaska, Fairbanks, Alaska,
- Marcot, B. G., M. T. Jorgenson, J. P. Lawler, C. M. Handel, and A. R. DeGange (2015), Projected changes in wildlife habitats in Arctic natural areas of northwest Alaska, Clim. Change, 130, 145-154, doi:10.1007/s10584-015-1354-x.



- McGuire, A. D., L. G. Anderson, T. R. Christensen, S. Dallimore, L. Guo, D. Hayes, M. Heimann, T. Lorenson, R. W. Macdonald, and N. Roulet (2009), Sensitivity of the carbon cycle in the Arctic to climate change, Ecol. Monogr., 79(4), 523-555, doi:10.1890/08-2025.1.
- Minke, M., N. Donner, N. Karpov, P. de Klerk, and H. Joosten (2009), Patterns in vegetation composition, surface height and thaw depth in polygon mires in the Yakutian Arctic (NE Siberia): A microtopographical characterisation of the active layer, Permafrost Periglac. Proc., 20, 357-368, doi:10.1002/ppp.663.
- Murton, J. B. (2013), Ground ice and cryostratigraphy, in Treatise on Geomorphology, edited by J. F. Shroder, pp. 173-201, Academic Press, San Diego, Calif.
- Nelson, F. E., N. I. Shiklomanov, K. M. Hinkel, and J. Brown (2008), Decadal results from the Circumpolar Active Layer Monitoring (CALM) program, in Proceedings of the Ninth International Conference on Permafrost, edited by K. M. Hinkel and D. L. Kane, pp. 1273–1280, Univ. of Alaska Press, Fairbanks, Alaska
- Osterkamp, T. E., M. T. Jorgenson, E. A. G. Schuur, Y. L. Shur, M. Z. Kanevsky, J. G. Vogel, and V. E. Tumskoy (2009), Physical and ecological changes associated with warming permafrost and thermokarst in Interior Alaska, Permafrost Perialac, Proc., 20, 235-256,
- Pollard, W. H., and H. M. French (1980), A first approximation of the volume of ground ice, Richards Island, Pleistocene Mackenzie Delta, Northwest Territories, Canada, Can. J. Earth Sci., 17, 509-516, doi:10.1139/t80-059.
- Post, E., U. S. Bhatt, C. M. Bitz, J. F. Brodie, T. L. Fulton, M. Hebblewhite, J. Kerby, S. J. Kutz, I. Stirling, and D. A. Walker (2013), Ecological consequences of sea-ice decline, Science, 341, 519-524, doi:10.1126/science.1235225.
- Pullman, E. R., M. T. Jorgenson, and Y. Shur (2007), Thaw settlement in soils of the Arctic Coastal Plain, Alaska, Arctic Antarct. Alpine Res., 39(3), 468-476.
- Raynolds, M. K., D. A. Walker, K. J. Ambrosius, J. Brown, K. R. Everett, M. Kanevskiy, G. P. Kofinas, V. E. Romanovsky, Y. Shur, and P. J. Webber (2014), Cumulative geoecological effects of 62 years of infrastructure and climate change in ice-rich permafrost landscapes, Prudhoe Bay Oilfield, Alaska, Global Change Biol., 20(4), 1211-1224, doi:10.1111/gcb.12500.
- Romanovskii, N. N. (1985), Distribution of recently active ice and soil wedges in the USSR, in Field and Theory: Lectures in Geocryology, edited by M. Church and O. Slaymaker, pp. 154–165, Univ. of British Columbia, Vancouver.
- Péwé, T. L. (1963), Ice wedges in Alaska; classification, distribution, and climatic significance, in Proceedings Permafrost International Conference, Natl. Res. Council Publ., 1287, pp. 76-81, Natl. Acad. of Sci.
- Sachs, T., M. Giebels, J. Boike, and L. Kutzbach (2010), Environmental controls on CH4 emission from polygonal tundra on the micro-site scale in the Lena River Delta, Siberia, Global Change Biol., 16(11), 3096-3110, doi:10.1111/j.1365-2486.2010.02232.x.
- Scenarios-Network-for-Arctic-Planning (2014), Regional climate projections, Univ. of Alaska Fairbanks. [Available at https://www.snap.uaf. edu/tools-and-data/all-analysis-tools.]
- Schuur, E. A. G., et al. (2015), Climate change and the permafrost carbon feedback, Nature, 520(7546), 171-179, doi:10.1038/nature14338. Screen, J. A., and I. Simmonds (2010), The central role of diminishing sea ice in recent Arctic temperature amplification, Nature, 464, 1334-1337, doi:10.1038/nature09051.
- Shiklomanov, N. I., D. A. Streletskiy, J. D. Little, and F. E. Nelson (2013), Isotropic thaw subsidence in undisturbed permafrost landscapes, Geophys. Res. Lett., 40, 6356-6361, doi:10.1002/2013GL058295.
- Shur, Y. L. (1988), The upper horizon of permafrost soil, in Proceedings of the Fifth Intern. Conf. on Permafrost, edited by K. Senneset, pp. 867-871, Tapir Publishers, Trondheim, Norway.
- Shur, Y. L., and M. T. Jorgenson (2007), Patterns of permafrost formation and degradation in relation to climate and ecosystems, Permafrost Perialac, Proc., 18, 7-19, doi:10.1002/ppp.582.
- Shur, Y., and T. E. Osterkamp (2007), Thermokarst, Rep. INE06.11, 50 pp., Institute of Northern Engineering, Univ. of Alaska Fairbanks, Fairbanks, Alaska,
- Shur, Y., K. M. Hinkel, and F. E. Nelson (2005), The transient layer: Implications for geocryology and climate-change science, Permafrost Periglac. Proc., 16(1), 5-17, doi:10.1002/ppp.518.
- Shur, Y., M. T. Jorgenson, and M. Z. Kanevskiy (2014), Permafrost, in Encyclopedia of Snow, Ice and Glaciers, edited by V. P. S. Singh et al., pp. 841-848, Springer, Netherlands.
- Steedman, A. E. (2014), The ecology and dynamics of ice wedge degradation in high-centre polygonal terrain in the uplands of the Mackenzie Delta region, Northwest Territories, MS thesis, Univ. of Victoria.
- Vtyurin, B. I. (1975), Ground Ice in the USSR [in Russian], Nauka, Moscow.
- Walker, D. A., K. R. Everett, P. J. Webber, and J. Brown (1980), Geobotanical Atlas of the Prudhoe Bay Region, Alaska, Rep. Laboratory Report 80-14, 69 pp., U.S. Army Corps of Engineers Cold Regions Research and Engineering, Hanover, N. H.
- Walvoord, M. A., and R. G. Striegl (2007), Increased groundwater to stream discharge from permafrost thawing in the Yukon River basin: Potential impacts on lateral export of carbon and nitrogen, Geophys. Res. Lett., 34, L12402, doi:10.1029/2007GL030216.